Photochemical & Photobiological Sciences

Cite this: *Photochem. Photobiol. Sci.*, 2011, **10**, 992

www.rsc.org/pps

PAPER

Mesogenic BODIPYs: an investigation of the correlation between liquid crystalline behaviour and fluorescence intensity†

Michael Benstead,[a] Geraldine A. Rosser,[b] Andrew Beeby,[b] Georg H. Mehl*[a] and Ross W. Boyle*[a]

Received 21st December 2010, Accepted 7th February 2011
DOI: 10.1039/c0pp00388c

A series of mesogenic molecules based on the 4,4′-difluoro-3a,4a-diaza-s-indacene (BODIPY) fluorophore have been synthesised and characterised. Each compound consists of one mesogenic unit, based on a cyanobiphenyl core, and one fluorophore, of varying alkyl substitution. The compounds were prepared by microwave-assisted palladium-catalyzed couplings (Suzuki and Sonogashira) due to slow reaction rates under conventional heating conditions. The effect of increasing the molecular length was also investigated by incorporating an ethynyl unit between the mesogen and the fluorophore. The molecules self-assemble into monotropic nematic phases which were identified by optical polarising microscopy (OPM) and differential scanning calorimetry (DSC). The compounds were found to display varying degrees of fluorescence quantum yield dependant on the number of alkyl substituents attached to the fluorophore. A relationship was observed between the nematic phase stability and fluorescence intensity of the compounds with increasing alkyl substitution causing an increase in fluorescence intensity due to restriction of the 8-phenyl ring rotation while simultaneously disrupting nematic phase formation, causing a reduction in nematic range. Temperature-dependant fluorescence measurements were also acquired along with fluorescence measurements of four of the synthesised BODIPYs dissolved in a commercial nematic liquid crystal (BL024) and incorporated into a twisted nematic cell.

Introduction

4-Difluoro-4-bora-3a,4a-diaza-*s*-indacene (BODIPY) derivatives are attracting at present increasing attention, primarily due to their remarkable photophysical properties. High fluorescence quantum yields, sharp absorption spectra, large molar extinction coefficients and excellent photostability[1] have prompted the intensive search for applications in both biological and materials science.[2–4] Fluorescent chemosensors,[5–8] laser dyes,[9,10] fluorescent labels,[11] photodynamic therapy[12] and electro-chemiluminescent materials[13–15] are some of the areas in which BODIPYs have so far been found to be useful.

One class of materials of particular interest are BODIPYs with liquid crystalline properties as they are able to exhibit various mesophases with differing degrees of molecular ordering that allow this extraordinary class of molecule to find applications in the expanding field of nanotechnology.[16] The use of BODIPYs as liquid crystalline materials, however, remains still relatively unexplored.[17–23] Due to liquid crystal mesophases being intermediates between crystals and isotropic liquids, the structure of any potential liquid crystalline molecule must be carefully designed in order to control the strength of the intermolecular interactions. The effect that attachment of the fluorescent BODIPY core has on the liquid crystalline behaviour of a mesogen has not, to the best of our knowledge, been systematically investigated.

While liquid crystalline dendrimers have been used to induce liquid crystallinity on BODIPYs,[18] our focus has been on using a well understood liquid crystalline mesogen in order to observe the effect that 'fine-tuning' the structure of a mesogenic BODIPY has on self-assembling behaviour. BODIPYs have been shown to exhibit columnar behaviour when a branched structure was attached to the BODIPY core so that the resulting molecule had a disc-like structure.[21] This columnar stacking is promoted by the tendency of the BODIPY core to aggregate in a similar way to porphyrins and phthalocyanines.[24–26] Our aim, however, was to investigate the calamitic mesogenic activity of BODIPYs. This approach was selected in order to make the systems more compatible with calamitic nematic liquid crystals, the class of materials that is incorporated in the majority of electronic devices that incorporate liquid crystalline materials

In this article we report the synthesis of two series of mesogenic BODIPYs and the liquid crystalline behaviour they display. The effect of using a different linker groups between the BODIPY core and mesogenic unit is explored, and the photophysical properties of the resulting BODIPYs are reported.

[a]*Department of Chemistry, University of Hull, Kingston-Upon-Hull, East Yorkshire, UK HU6 7RX. E-mail: r.w.Boyle@hull.ac.uk, g.h.mehl@hull.ac.uk; Fax: +44(0)1482 466410; Tel: +44(0)1482 466353*

[b]*Department of Chemistry, Durham University, Durham, DH1 3LE, UK*

† Electronic supplementary information (ESI) available: Synthetic procedures, DSC thermograms, NMR spectra, HRMS profiles, HPLC traces. See DOI: 10.1039/c0pp00388c

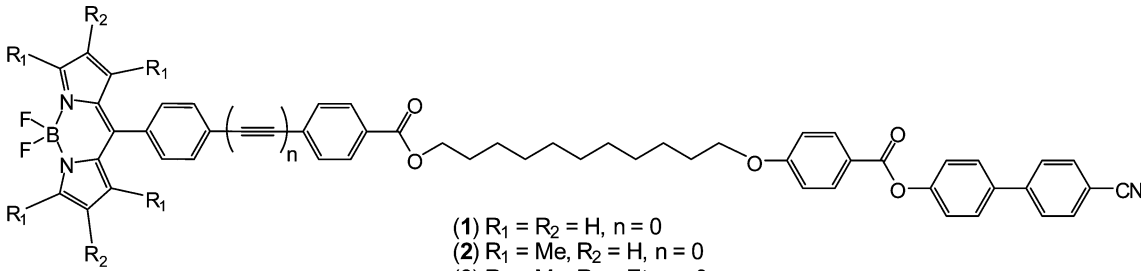

Fig. 1 Mesogenic BODIPYs.

Results and discussion

Synthesis

The target BODIPYs (Fig. 1) were synthesised *via* a convergent method. Firstly, BODIPYs which terminated in either an iodo- or ethynyl-group were synthesised in order to allow mesogen attachment *via* palladium-catalyzed cross-couplings (either Suzuki or Sonogashira couplings[27]). The purpose of incorporating an ethynyl group onto the BODIPY was to investigate the effect that lengthening the long molecular axis of the subsequent mesogenic BODIPY had on the liquid crystal properties of the compound.

BODIPY **A** (Fig. 2) was prepared *via* a one-pot synthesis involving formation of the dipyrromethane with subsequent oxidation using DDQ to form the dipyrrin before complexation of the borondifluoro moiety (Scheme 1). This yielded the desired BODIPY in an overall yield of 6% after chromatography.

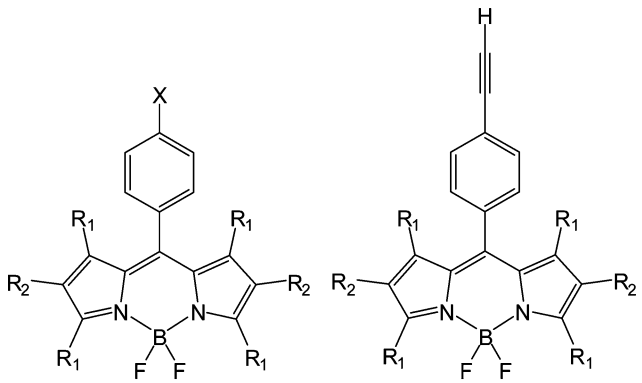

Fig. 2 BODIPYs suitable for mesogen attachment *via* palladium-catalyzed couplings.

BODIPYs **B** and **C** were prepared by an alternative route involving preparation (but not isolation) of the dipyrrin hydrochloride salt by refluxing the appropriate pyrrole in the presence of 4-iodobenzoyl chloride (Scheme 2) before borondifluoro complexation. This approach eliminates the dipyrromethane formation step, thus improving yields and simplifying purification due to fewer side-products being present. These compounds were isolated in very similar yields of 35% and 36% for **B** and **C**, respectively, after chromatography.

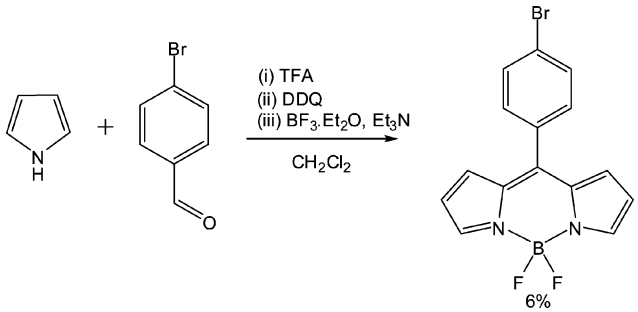

Scheme 1 One-pot synthesis of BODIPY **A** from pyrrole and 4-bromobenzaldehyde.

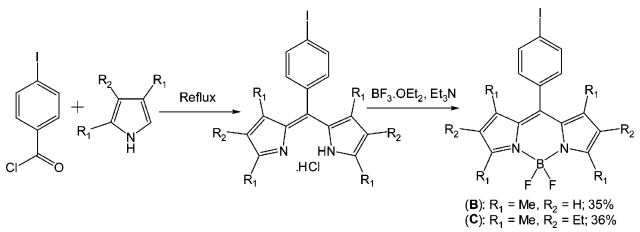

Scheme 2 One-pot synthesis of B and C from their respective pyrrolic precursors and 4-iodobenzoyl chloride.

Compounds **D–F** were prepared *via* an analogous route to that employed for the preparation of compound **A**, involving pyrrole and 4-[(trimethylsilyl)ethynyl]benzaldehyde (Scheme 3). The TMS-protected precursors to **D** and **E** were isolated and

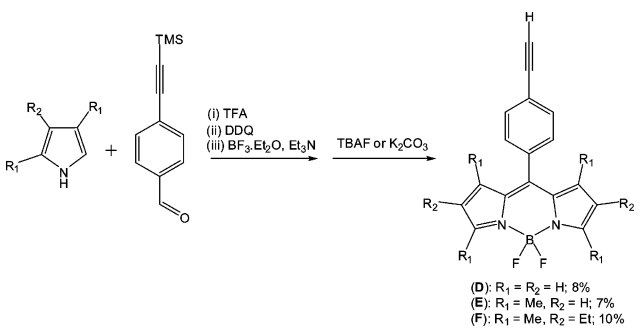

Scheme 3 One-pot synthesis of TMS-protected BODIPY with subsequent deprotection.

characterized before deprotection, while facile deprotection of **F** during purification made isolation of the protected form difficult. This was overcome by reacting the impure mixture with potassium carbonate to fully deprotect the BODIPY in order to isolate compound **F**. Deprotection was achieved using either potassium carbonate or TBAF, however it was found that partial decomposition of the BODIPY occurred when TBAF was employed as the deprotecting agent.

The mesogenic units (**G** and **H**) were obtained in reasonable yields in three steps starting form 4-hydroxybenzoic acid and 11-bromoundecan-1-ol. The final step in the mesogen synthesis was the attachment of the subunit with the reactive site for subsequent palladium-catalyzed coupling to the BODIPY (Scheme 4). No chromatography was required in the purification of the mesogens with recrystallisation yielding the pure compounds.

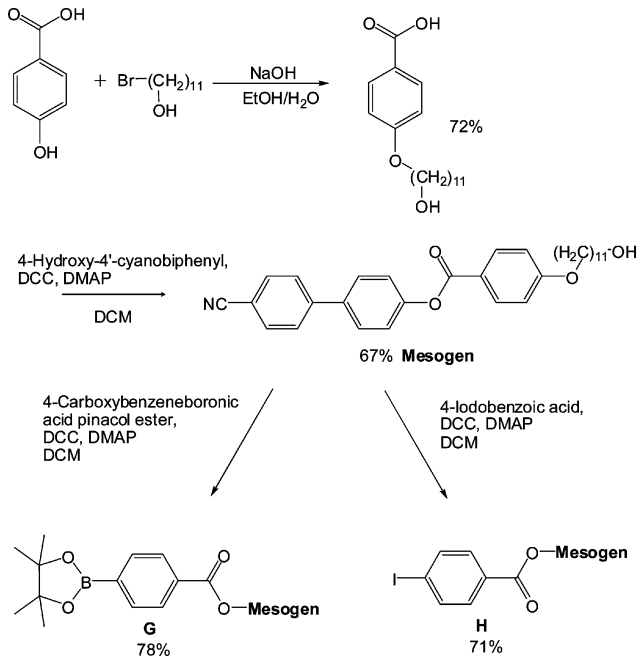

Scheme 4 Mesogen synthesis.

Attachment of the mesogen was then achieved by microwave-assisted palladium-catalyzed carbon-carbon bond formation (Schemes 5 and 6). While both Suzuki and Sonogashira couplings involving BODIPYs have been previously published using conventional heating methods,[27,28] we found that attaching a large substituent, like the mesogen, to the BODIPY under these conditions proved to be a very slow reaction (4–5 days) which gave poor yields (<10%). The microwave-assisted reaction, however, went to completion in just 5 min. Purification involved removal of the solvent followed by chromatography. Subsequent precipitation from either ethyl acetate or DCM with MeOH removed any trace impurities from the desired product, the impurities being unreacted mesogen which eluted at a similar rate to the mesogenic BODIPY product in some cases. The yields for the Suzuki and Sonogashira reactions were moderate, with **2** producing the highest yield (49%) and **1** the lowest (20%) of the two series with the Sonogashira reactions in particular giving quite similar yields.

Originally, the BODIPY containing an iodo-functionality was reacted with 4-carboxyphenylboronic acid pinacol ester under

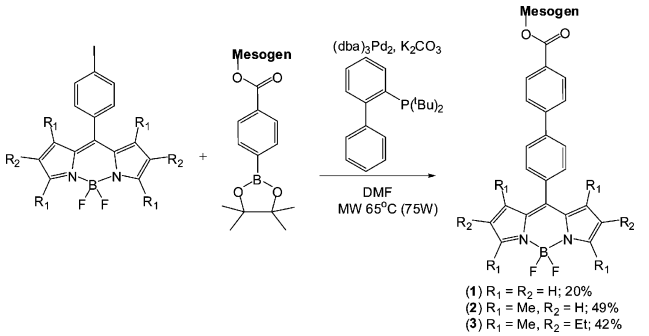

Scheme 5 Mesogen attachment by microwave-assisted Suzuki-coupling.

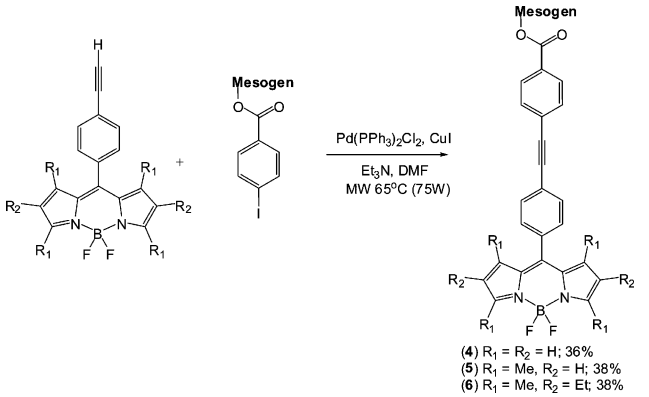

Scheme 6 Mesogen attachment by microwave-assisted Sonogashira-coupling.

Suzuki-coupling conditions in order to produce a BODIPY terminating in a carboxy-group, which would then be reacted with the mesogenic group (terminating in a hydroxyl group) *via* carbodiimide (DCC) mediated coupling. We found, however, that the DCC-coupling was sluggish (3 days) and gave poor yields (<10%). This was attributed to the mesogenic group containing an alkyl hydroxy group and being a relatively large substituent, which led us to the routes used in Scheme 5 and 6 for mesogen attachment, due to the improved reaction rates and yields. The molecular structures and purity were assigned by ^{1}H and ^{13}C-NMR spectroscopy, mass spectrometry and HPLC analysis. An attempt was also made to carry out a Heck reaction under similar conditions as the Suzuki coupling in order to attach a mesogenic unit *via* a third linker group but this reaction was found to be unsuccessful.

Liquid crystal properties

The liquid crystalline properties of compounds **1–6** were investigated by optical polarizing microscopy (OPM) and differential scanning calorimetry (DSC) (Fig. 3–6). Compounds **1**, **2** and **4** displayed mesophase behaviour while **3**, **5** and **6** displayed traditional melting behaviour. The liquid crystal and thermodynamic data are reported in Table 1.

As can be seen from Table 1, compounds **1**, **2** and **4** all display monotropic nematic phases. Compounds **1** and **2** both exhibit the schlieren texture (Fig. 5 and 6) typical of nematic liquid crystals when cooled down from the isotropic liquid into the nematic phase. Compound **1** exhibits a nematic phase over 21 °C and the melting point is about 3 °C higher than the

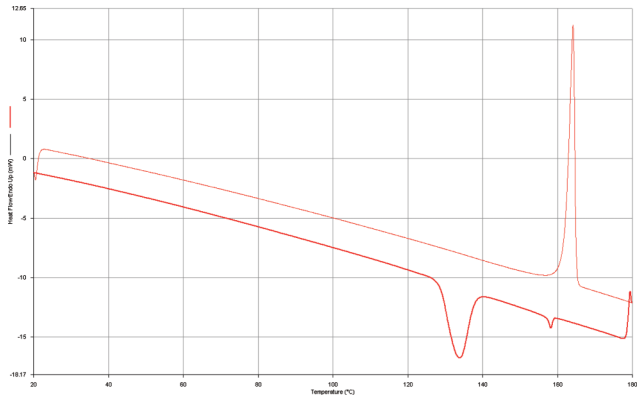

Fig. 3 DSC thermogram of compound **1** showing second heat (top) and cool (bottom).

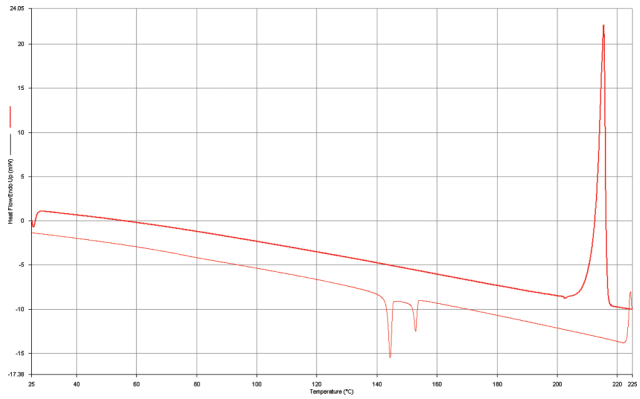

Fig. 4 DSC thermogram of compound **2** showing second heat (top) and cool (bottom).

isotropisation temperature, but when the BODIPY core is made bulkier (compound **2**) the nematic range is shortened to 8 °C and the material needs to be supercooled by 58 °C below the melting point to achieve mesomorphic behaviour. We attribute this to the four additional methyl units on the BODIPY core disrupting the molecular packing of the nematic phase. This effect is reinforced in compound **3** in which the BODIPY core contains an additional two ethyl groups, further increasing the bulk of the fluorophore. The alkyl groups further enhance the disruption in the molecular packing, destabilizing the nematic phase enough for it to disappear completely. The DSC thermogram of compound **2** (Fig. 4) also shows that it has to be supercooled by 58 °C before exhibiting the nematic phase. The reduced entropies ($\Delta S/R$) were calculated in order to compare the relative enthalpy and entropy changes associated with each compound. The reduced entropies for compound **1** and **4** were found to be quite similar, while that of

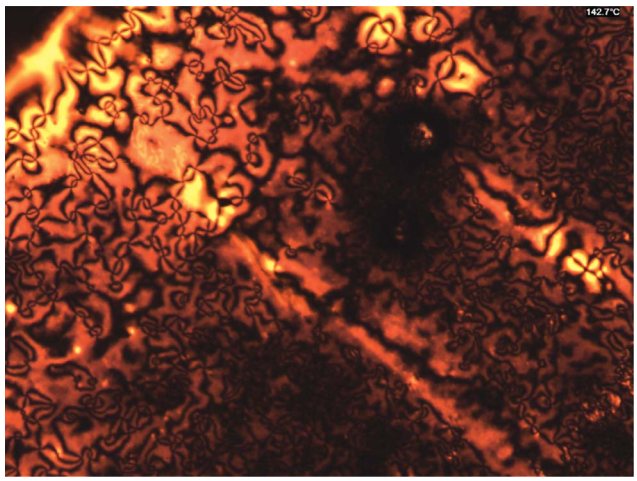

Fig. 5 OPM image of compound **1** in the nematic phase at 142.7 °C.

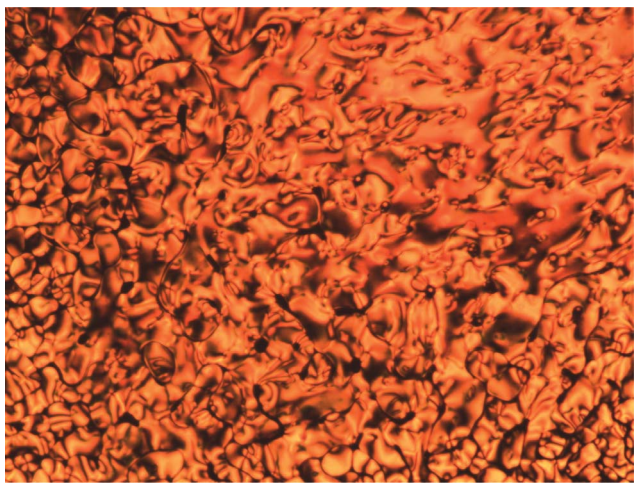

Fig. 6 OPM image of compound **2** in the nematic phase at 148.6 °C.

compound **2** was noticeably higher indicating that the four methyl groups have a distinct effect on the melting process as well as on the melting points.

Compound **4** is analogous to compound **1** in that they contain the same fluorophore; however, compound **4** has an extended molecular length due to the incorporation of an acetylinic unit between the fluorophore and the mesogen. As shown in Fig. 7, compound **4** displays the typical schlieren texture of a nematic phase. As can be seen from Table 1, the melting point is increased to 183 °C; this is an increase of 21 °C when **1** and **4** are compared, the nematic phase of compound **4** has been shortened relative to compound **1** (21 °C to 7 °C). Moreover the DSC thermogram of compound **4** (Fig. 8) shows that it needs be supercooled by 17 °C

Table 1 Phase transitions, nematic ranges, Iso-N enthalpy changes and reduced entropies for mesogenic BODIPYs

Compound	LC transitions/°C	Nematic range/°C	ΔH/kJ mol^{-1} (Iso-N transition)	$\Delta S_{mol}/R$ (Iso-N transition)
1	Cr (N 159) 162 I	21	1.54	0.43
2	Cr (N 153) 211 I	8	4.12	1.15
3	m.p 192–194 °C	—	—	—
4	Cr (N 166) 183 I	7	0.86	0.24
5	m.p. 199–200 °C	—	—	—
6	m.p. 184–185 °C	—	—	—

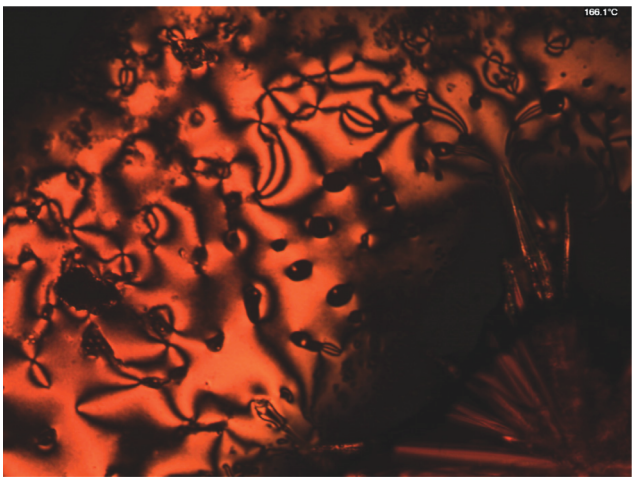

Fig. 7 OPM image of compound **4** in the nematic phase at 166.1 °C.

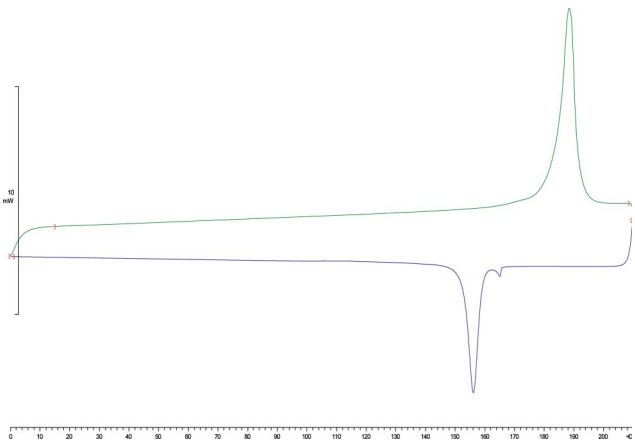

Fig. 8 DSC thermogram of compound **4** showing second heat (top) and cool (bottom).

before exhibiting the nematic phase, this compares to 3 °C for **1**. Altogether this means that the liquid crystalline properties of **4**, where the long axis of the molecule is increased, are poorer than those of the smaller analogue **1**. While increasing the molecular length of the mesogenic BODIPY is unlikely to disrupt molecular packing, it is likely that the increased length is actually enhancing the molecular packing causing the molecule to have an increased preference for crystalline behaviour due to increased van der Waals and π–π interactions. In going from compound **4** to compound **5**, a similar effect is seen as for compound **1** to **2**. The increased bulk around the fluorophore causes disruption in the molecular packing and elimination of the nematic phase.

Photophysical studies

Table 2 shows the spectroscopic data for compounds **1–6**. All the compounds show fluorescence spectra characteristic of BODIPY fluorophores. The absorption spectra show strong $S_0 \rightarrow S_1$ ($\pi \rightarrow \pi^*$) transitions between 505–530 nm. Normalized spectra for BODIPYs **1–3** and **4–6** are shown in Fig. 9 and 10 respectively.

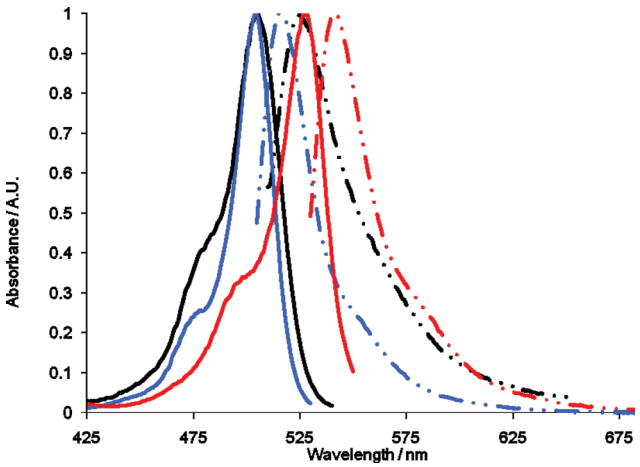

Fig. 9 Excitation (solid line) and emission (dashed line) of compounds **1** (black), **2** (blue) and **3** (red) in toluene at 298 K.

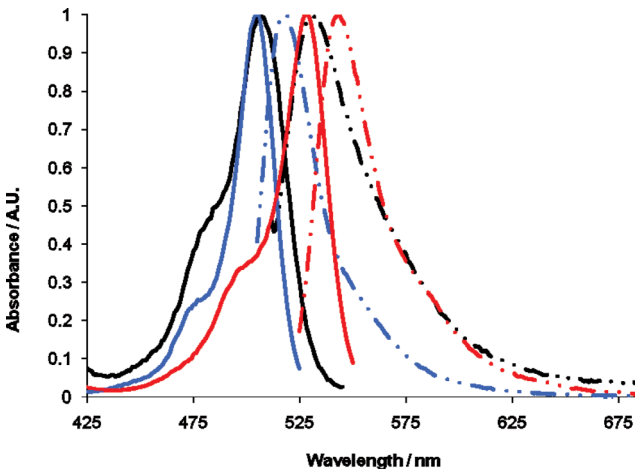

Fig. 10 Excitation (solid line) and emission (dashed line) of compounds **4** (black), **5** (blue) and **6** (red) in toluene at 298 K.

The fundamental photophysical properties of BODIPYs have been extensively studied previously and the compounds presented herein exhibit fluorescence profiles similar to those of previously reported BODIPYs bearing an 8-phenyl ring.[29,30] Compounds **1–6**

Table 2 Spectroscopic data of mesogenic BODIPYs **1–6** measured in toluene or CH_2Cl_2 at 298 K

Compound	λ_{ex}/nm	λ_{em}/nm	Φ_F	ε/M^{-1} cm^{-1}	ΔS/nm	τ_F/ns
1	505	526	0.032	57000	21	0.18
2	505	517	0.48	89000	12	2.66
3	528	543	0.63	103000	15	2.18
4	508	533	0.01	116000	25	<0.1
5	506	519	0.37	92000	13	2.27
6	529	544	0.78	82000	15	4

Table 3 Structure-property relationship between fluorescence intensity and liquid crystallinity

Compound	LC transitions/°C	Nematic range/°C	Φ_F
1	Cr (N 159) 162 I	21	0.032
2	Cr (N 153) 211 I	8	0.48
3	—	—	0.63
4	Cr (N 166) 183 I	7	0.01
5	—	—	0.37
6	—	—	0.78

show varying degrees of fluorescence intensity dependant on the alkyl substituents present on the BODIPY core. The increases in fluorescence quantum yield being caused by increased rotational restriction of the 8-phenyl ring as is well-known for BODIPY chromophores.[31,32] The increase in fluorescence intensity from compound **2** to **3** and **5** to **6** is more likely to be due to electronic effects, as the ethyl group is not large enough to interact efficiently with the 8-phenyl ring. The fluorescence lifetimes of the mesogenic BODIPYs vary quite widely between the less and more sterically hindered fluorophores. Compounds **1** and **4**, which contain no alkyl substituents on the BODIPY core, have particularly short lifetimes (0.18 and <0.1 ns, respectively). We attribute these short lifetimes to the increased preference of the molecule to lose energy by non-radiative processes as well as a small amount by fluorescent processes. All the mesogenic BODIPYs have similar excitation and emission wavelengths, with those of compounds **3** and **6** being slightly red-shifted. Compounds **1–3** display a gradual increase in absorption coefficient with increasing alkyl substitution while compounds **4–6** display a gradual decrease. All of the calculated absorption coefficients are comparable to those for previously reported BODIPYs.

Structure-property relationship between fluorescence intensity and liquid crystallinity

As can be seen from Table 3, there is a distinct relationship between the fluorescence intensity and nematogenicity of compounds **1–6**. As seen in previously reported BODIPYs, restricting the rotation of the 8-phenyl ring results in an increase in fluorescence quantum yield due to a reduction in non-radiative de-excitation processes. This effect is clearly seen in series **1–3** and **4–6**.

While increasing substitution of the BODIPY core has a very predictable effect on the fluorescence quantum yield, the effect it has on any potential liquid crystalline behaviour is not quite so obvious due to the lack of investigation in this particular aspect of BODIPYs.

Due to the BODIPY fluorophore being in a terminal position on the molecule, increased alkyl substitution only increases the size of one terminal while the other (mesogenic) terminal remains constant. By attaching four methyl units (**2** and **5**) we observed quite a dramatic increase in melting point along with a reduction in nematic range, when compared to the unsubstituted analogues (**1** and **4**). In the case of compounds **3** and **5**, the nematic phase is disrupted sufficiently for it to disappear completely. Calamitic liquid crystals have been shown to display decreased melting points when lateral alkyl substituents are attached, implying that the four methyl groups in compounds **2** and **5** do not cause a dramatic reduction in the length-to-breadth ratio of the molecule. This effect is also observed in compound **5** which, despite the lack of nematic behaviour, has a higher melting point (199–200 °C) than unsubstituted analogue **4**. The four methyl substituents appear to be promoting crystalline behaviour by disrupting the nematic phase packing due to additional intermolecular steric interactions. Along with this reduction in nematic range, the four methyl groups provide a dramatic increase in fluorescence intensity from compounds **1** to **2** and **4** to **5**.

This effect is also observed in compounds **3** and **6**. By attaching ethyl substituents to the BODIPY core the length-to-breadth ratio has been reduced, causing a reduction in melting point when compared to the previous BODIPY in the series, and in the case of **3** the disappearance of the nematic phase completely. This could be due to the relatively large ethyl groups stabilising either the crystalline or isotropic liquid phase over the nematic phase. The ethyl groups also cause a further increase in fluorescence quantum yield due to a slightly longer range steric effect on the 8-phenyl ring, causing further rotational restriction. The increase in fluorescence intensity of these compounds is, however, not as marked as compounds **1** to **2** and **4** to **5**.

We have shown here that there is a clear inverse relationship between fluorescence intensity and liquid crystallinity for these two series of compounds. While this is the first study of the effect alkyl substitution on the BODIPY core has on the liquid crystalline behaviour of this type of calamitic molecule, it would be reasonable to assume that a similar effect would be observed in other series of mesogenic BODIPYs with a similar shape.

Temperature-dependant fluorescence measurements and BODIPY-doped nematic liquid crystal fluorescence

Compound **1** was chosen to carry out temperature-dependant fluorescence measurements as it exhibited the widest nematic range of the compounds synthesised herein. It has been reported previously that the fluorescence of a liquid crystalline BODIPY increases with decreasing temperature,[18] which is an effect observed in this case also. However, no marked increase in fluorescence intensity was reported upon transition from the isotropic to the nematic phase or from the nematic to the crystalline phase. In the case of compound **1**, while no significant increase in fluorescence intensity is observed in the transition from the isotropic liquid to the nematic phase, a noticeable increase in fluorescence intensity occurs when cooling from 150 °C to 140 °C (Fig. 11). As can

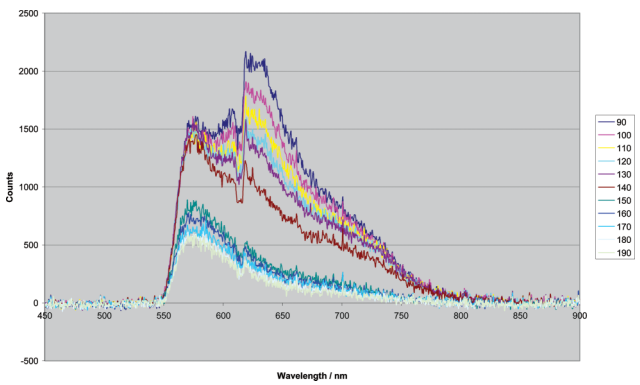

Fig. 11 Temperature-dependant fluorescence measurements of compound **1** at 10 °C intervals (heated to 190 °C and cooling down to 90 °C; see legend) excited with a Nd:YAG laser.

be seen from the DSC thermogram of compound **1** (Fig. 3), crystallisation from the nematic phase into the crystalline phase starts to occur around 140 °C and a short time annealing the sample allows almost complete crystallisation to occur. This causes the molecules to adopt a much more rigid conformation, presumably greatly restricting the rotation of the 8-phenyl ring while also causing a reduction in other molecular motions causing an increase in fluorescence intensity. Decreasing the temperature in the crystalline phase causes an increase in fluorescence intensity from a second emission maximum at approximately 620 nm, corresponding to the increased formation of *J*-dimers as the molecules pack closer together. This peak is only slight when in the isotropic or nematic phase due to the more diffuse nature of the molecular packing. The formation of aggregates does occur to a certain extent as evidenced by the red-shift in the fluorescence compared to the solution-based measurements but is much more pronounced when crystallisation occurs. It was expected that the transition from the isotropic to the nematic phase would also cause an increase in fluorescence intensity due to increased 8-phenyl ring rotational restriction but this was not observed, presumably due to the more diffuse nature of a nematic phase over a layered phase *e.g.* smectic, or the crystalline phase.

In order to investigate the effect that the alignment of the BODIPY molecules has on their fluorescence, four of the mesogenic BODIPYs (**1**, **3**, **4** and **6**) were dissolved (0.3 weight%) in a commercial nematic liquid crystal (BL024 – Merck) and incorporated into a twisted nematic cell (inner top plate aligned perpendicular to the bottom plate). The sample was excited with a UV laser and the fluorescence intensity was measured when an electric field was applied. Compounds **1**, **3**, **4** and **6** were chosen as they were the most and least fluorescent compounds of their respective series (Fig. 12–15). Compounds **4** and **6** were studied to investigate if the increased molecular length had any effect on the alignment with the host material.

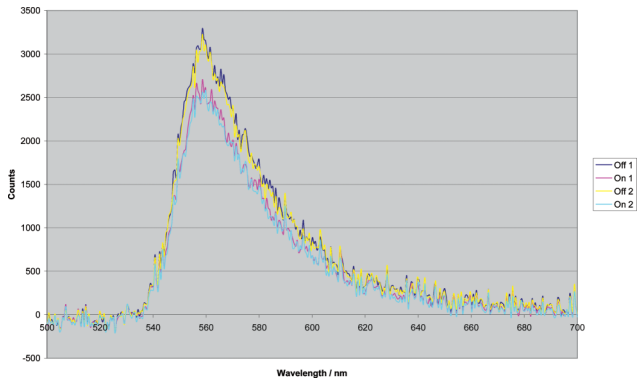

Fig. 12 Fluorescence intensity of compound **1** dissolved in BL024 in a twisted nematic cell (two measurements taken with an electric field applied (On) and two without an electric field applied (Off); see legend). Maximum at 559 nm.

The core-unsubstituted mesogenic BODIPYs only displayed a minor change in fluorescence intensity when the electric field was applied. In particular, the mixture of compound **4** displayed no obvious change in fluorescence intensity (Fig. 14). The mixture of compound **1**, however, displayed a small, but noticeable, reduction in fluorescence intensity when the electric field was applied (Fig. 12). While moderate changes in the fluorescence intensity of the dye molecules are observed, without performing additional experiments into the polarisation of the emitted light from the cell, a definitive explanation for these effects is difficult to attain.

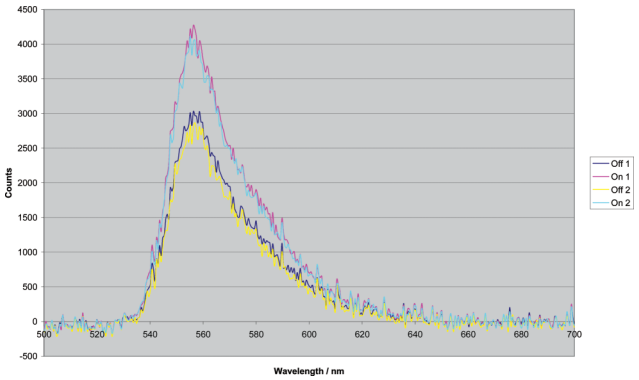

Fig. 13 Fluorescence intensity of compound **3** dissolved in BL024 in a twisted nematic cell (two measurements taken with an electric field applied (On) and two without an electric field applied (Off); see legend). Maximum at 556 nm.

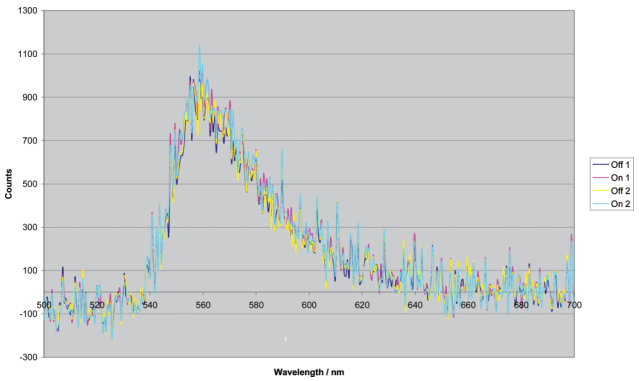

Fig. 14 Fluorescence intensity of compound **4** dissolved in BL024 in a twisted nematic cell (two measurements taken with an electric field applied (On) and two without an electric field applied (Off); see legend). Maximum at 559 nm.

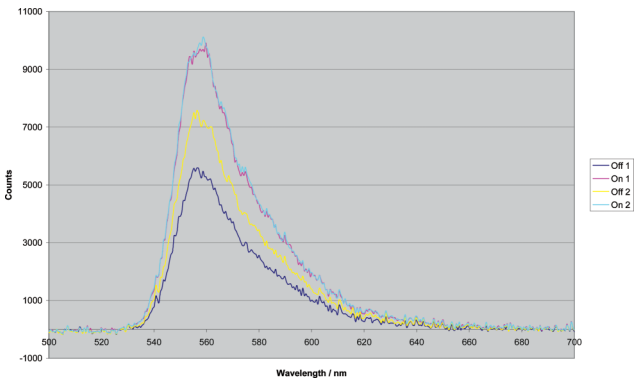

Fig. 15 Fluorescence intensity of compound **6** dissolved in BL024 in a twisted nematic cell (two measurements taken with an applied electric field (On) and two without an applied electric field (Off); see legend). Maximum at 559 nm.

Conclusions

BODIPY fluorophores have been successfully attached to mesogenic substituents by palladium-catalyzed couplings. Two series of mesogenic BODIPYs were synthesised and their interesting fluorescence and liquid crystalline behaviour was observed. We have also displayed the effect that a different linker group has on the liquid crystalline behaviour of mesogenic BODIPYs. While the fluorescence quantum yields increased through the two series quite predictably, the liquid crystallinity decreased with increasing substitution of the BODIPY core. We attributed this to the increased steric bulk of the fluorophore causing a preference for crystalline behaviour over liquid crystallinity due to increased intermolecular steric interactions. This is the first reported observation of the inverse relationship between fluorescence quantum yield and liquid crystallinity of mesogenic BODIPYs. The fluorescence of one of the prepared BODIPYs was also measured relative to its temperature and it was found that, while a gradual increase in intensity was observed with decreasing temperature, no significant change was observed in the isotropic liquid to nematic transition. However, a larger increase in intensity was observed in the nematic to crystalline transition due to the molecules adopting a much more rigid configuration. Fluorescence measurements were also acquired of several of the compounds dissolved in a nematic host material and incorporated into a twisted nematic cell. The application of an electric field caused alterations in the observed fluorescence intensity, possibly due to the shifting alignment of the dye molecules relative to the excitation beam. While further experimentation is required to explain this effect, it is of particular relevance in the context of nanotechnology, specifically supramolecular electronic display devices.

References

1 R. P. Haugland, *Handbook of Fluorescent Probes and Research Chemicals*, 6th edn, Molecular Probes, Eugene, OR, 1996.
2 R. Ziessel, G. Ulrich and A. Harriman, *New J. Chem.*, 2007, **31**, 496–501.
3 A. Loudet and K. Burgess, *Chem. Rev.*, 2007, **107**, 4891–4932.
4 G. Ulrich, R. Ziessel and A. Harriman, *Angew. Chem., Int. Ed.*, 2008, **47**, 1184–1201.
5 R. W. Wagner and J. S. Lindsey, *Pure Appl. Chem.*, 1996, **68**, 1373–1380.
6 M. Baruah, W. Qin, N. Basarić, W. M. De Borggraeve and N. Boens, *J. Org. Chem.*, 2005, **70**, 4152–4157.
7 M. Baruah, W. Qin, C. Flors, J. Hofkens, R. A. L. Vallée, D. Beljonne, M. Van Der Auweraer, W. M. De Borggraeve and N. Boens, *J. Phys. Chem. A*, 2006, **110**, 5998–6009.
8 S. Yin, V. Leen, S. V. Snick, N. Boens and W. Dehaen, *Chem. Commun.*, 2010, **46**, 6329–6331.
9 T. Chen, J. H. Boyer and M. L. Trudell, *Heteroat. Chem.*, 1997, **8**, 51–54.
10 G. Sathyamoorthi, J. H. Boyer, T. H. Allik and S. Chandra, *Heteroat. Chem.*, 1994, **5**, 403–407.
11 G. Ulrich, C. Goze, M. Guardigli, A. Roda and R. Ziessel, *Angew. Chem., Int. Ed.*, 2005, **44**, 3694–3698.
12 S. Atilgan, Z. Ekmekci, A. L. Dogan, D. Guc and E. U. Akkaya, *Chem. Commun.*, 2006, 4398–4400.
13 R. Y. Lai and A. J. Bard, *J. Phys. Chem. B*, 2003, **107**, 5036–5042.
14 J. M. Brom and J. L. Langer, *J. Alloys Compd.*, 2002, **338**, 112–115.
15 A. Hepp, G. Ulrich, R. Schmechel, H. Von Seggern and R. Ziessel, *Synth. Met.*, 2004, **146**, 11–15.
16 T. Kato, N. Mizoshita and K. Kishimoto, *Angew. Chem., Int. Ed.*, 2006, **45**, 38–68.
17 C. J. Wilson, L. James, G. H. Mehl and R. W. Boyle, *Chem. Commun.*, 2008, 4582–4584.
18 S. Frein, F. Camerel, R. Ziessel, J. Barbera and R. Deschenaux, *Chem. Mater.*, 2009, **21**, 3950–3959.
19 J. H. Olivier, F. Camerel, G. Ulrich, J. Barbera and R. Ziessel, *Chem.–Eur. J.*, 2010, **16**, 7134–7142.
20 F. Camerel, L. Bonardi, M. Schmutz and R. Ziessel, *J. Am. Chem. Soc.*, 2006, **128**, 4548–4549.
21 F. Camerel, L. Bonardi, G. Ulrich, L. Charbonniare, B. Donnio, C. Bourgogne, D. Guillon, P. Retailleau and R. Ziessel, *Chem. Mater.*, 2006, **18**, 5009–5021.
22 L. Bonardi, H. Kanaan, F. Camerel, P. Jolinat, P. Retailleau and R. Ziessel, *Adv. Funct. Mater.*, 2008, **18**, 401–413.
23 F. Camerel, G. Ulrich, J. BarberÃ- and R. Ziessel, *Chem.–Eur. J.*, 2007, **13**, 2189–2200.
24 N. Usol'Tseva, V. Bykova, N. Zharnikova, A. Alexandrov, A. Semeikin and A. Kazak, *Mol. Cryst. Liq. Cryst.*, 2010, **525**, 184–193.
25 A. E. Ahsen, A. Segade, D. Velasco and Z. Z. Aztark, *J. Porphyrins Phthalocyanines*, 2009, **13**, 1188–1195.
26 C. M. Drain, A. Varotto and I. Radivojevic, *Chem. Rev.*, 2009, **109**, 1630–1658.
27 T. Rohand, W. Qin, N. Boens and W. Dehaen, *Eur. J. Org. Chem.*, 2006, 4658–4663.
28 C. Thivierge, R. Bandichhor and K. Burgess, *Org. Lett.*, 2007, **9**, 2135–2138.
29 W. Qin, M. Baruah, M. Van Der Auweraer, F. C. De Schryver and N. Boens, *J. Phys. Chem. A*, 2005, **109**, 7371–7384.
30 W. Qin, T. Rohand, W. Dehaen, J. N. Clifford, K. Driesen, D. Beljonne, B. Van Averbeke, M. D. Van Auweraer and N. Boens, *J. Phys. Chem. A*, 2007, **111**, 8588–8597.
31 R. Bandichhor, C. Thivierge, N. S. P. Bhuvanesh and K. Burgess, *Acta Crystallogr., Sect. E: Struct. Rep. Online*, 2006, **62**, o4310–o4311.
32 E. V. d. Wael, J. A. Pardoen, J. A. V. Koeveringe and J. Lugtenburg, *Recl. Trav. Chim. Pays-Bas*, 1977, **96**, 306.